

V.F.2 The Effect of Airborne Contaminants on Fuel Cell Performance and Durability

Jean St-Pierre (Primary Contact), Yunfeng Zhai, Junjie Ge, Tatyana Reshetenko, Michael Angelo, Trent Molter¹, Leonard Bonville¹, Ugur Pasaogullari¹, Xiaofeng Wang¹, Jing Qi¹, Ozan Ozdemir¹, Amman Uddin¹, Navvab Khajeh-Hosseini-Dalasm¹, Jaehyung Park¹, Selvarani Ganesan¹, William Collins², Silvia Wessel³, Tommy Cheng³

Hawaii Natural Energy Institute
1680 East-West Road
Honolulu, HI 96822
Phone: (808) 956-3909
Email: jsp7@hawaii.edu

DOE Managers

Nancy Garland
Phone: (202) 586-5673
Email: Nancy.Garland@ee.doe.gov

Reg Tyler
Phone: (720) 356-1805
Email: Reginald.Tyler@ee.doe.gov

Technical Advisor

Tom Benjamin
Phone: (630) 252-1632
Email: benjamin@anl.gov

Contract Number: DE-EE0000467

Subcontractors

¹ University of Connecticut, Storrs, CT
² WPCSOL, East Windsor, CT
³ Ballard Power Systems, Burnaby, BC, Canada

Project Start Date: April 1, 2010
Project End Date: March 31, 2015

Overall Objectives

- Identify and mitigate the adverse effects of airborne contaminants on fuel cell system performance and durability
- Provide contaminants and tolerance limits for filter specifications (preventive measure)
- Identify fuel cell stack's material, design, operation or maintenance changes to remove contaminant species and recover performance (recovery measure)

Fiscal Year (FY) 2014 Objectives

Quantify spatial variability of performance loss and identify principal poisoning mechanism for at least four different contaminants.

Technical Barriers

This project addresses the following technical barriers from the Fuel Cells section of the Fuel Cell Technologies Office Multi-Year Research, Development, and Demonstration Plan:

- (A) Durability
- (B) Cost
- (C) Performance

Technical Targets

The following 2017 technical targets for automotive applications, 80-kW_e (net) integrated transportation fuel cell power systems operating on direct hydrogen, are considered:

- Durability: 5,000 hours in automotive drive cycle
- Cost: \$30/kW_e
- Performance: 60% energy efficiency at 25% of rated power

The effects of specific airborne contaminants are studied including a commercially relevant low-cathode-catalyst loading and the resulting information will be used to impact both preventive measures and recovery procedures:

- Airborne contaminant tolerance limits to support the development of filtering system component specifications and ensure negligible fuel cell performance losses
- Fuel cell stack material, design, operation, or maintenance changes to recover performance losses derived from contamination mechanisms

FY 2014 Accomplishments

- Completed characterization database using ex situ and in situ diagnostic techniques for seven airborne contaminants and one foreign cation to support the development of contamination mechanisms and recovery procedures that diminish the contamination impact on system durability and performance
- Assessed the effect of a decrease in cathode catalyst loading from 0.4 to a commercially relevant 0.1 mg Pt cm⁻² on the steady-state cell voltage loss during contamination for seven airborne contaminants

- Developed a transient, one-dimensional, through the membrane/electrode assembly plane model for foreign cation contamination to isolate individual cell performance effects which are not experimentally accessible and advance the understanding of contamination mechanisms
- Evaluated and modeled the scavenging effect of product liquid water for two cases, contaminant dissolution and contaminant dissolution followed by dissociation reactions, to determine effective contaminant concentrations within the cell and increase the accuracy of cell performance loss correlations



INTRODUCTION

The composition of atmospheric air cannot be controlled and typically includes contaminants, volatile compounds, as well as ions entrained by liquid water drops in the form of rain, mist, etc., especially near marine environments. Proton exchange membrane fuel cells operated with ambient air are therefore susceptible to deleterious effects which include decreased cell performance and durability [1,2]. Numerous air contaminants have not yet been tested in fuel cells and consequently their effects as well as recovery methods are unknown [2,3]. Furthermore, prevention is difficult to achieve because tolerance limits are also missing in most cases [2]. This increases the risk of failure for fuel cell systems and thus jeopardizes their introduction into the market.

Airborne contaminants and foreign ions have previously been selected using a cost-effective two-tiered approach combining qualitative and quantitative criteria [3]. Automotive fuel cells are used under a wide range of operating conditions resulting from changes in power demands (drive cycle). Temperature and current density impact fuel cell contamination the most [4]. The effect of contaminant concentration is also particularly important. Contaminant threshold concentrations for predetermined fuel cell performance losses were determined [5] to facilitate the definition of air filtering system tolerances (prevention). The effect of inlet reactant relative humidity is linked to the presence of liquid water within the cell which in turn may affect the effective contaminant concentration by dissolution and entrainment in water drops. This scavenging effect has not previously been considered. Cell design parameters also impact the severity of contamination. However, the effect of catalyst loading, which is important for cost reduction, has only been determined for a few species [2]. It is likely that prevention will be insufficient to avert all contaminant effects. Therefore, recovery procedures will also be needed, and these are more easily devised by understanding the origins of the contaminant effects (mechanisms). However

for the case of foreign cations, present experimental methods are insufficient to separate the different contributions to cell performance loss (thermodynamic, kinetic, ohmic, mass transport) [2,6,7]. Mathematical modeling is a valuable substitute approach. However, existing models either need improvement [8] or are incomplete. A separation factor more accurately represents ion exchange processes [9,10] and the change in oxygen permeability in the ionomer due to the presence of a foreign cation has not previously been tackled [11,12].

APPROACH

Impedance spectroscopy was first used to classify airborne contaminant effects into different resistance losses to focus subsequent activities. As a second step, more detailed information was obtained using other diagnostics methods to unravel contamination mechanisms: rotating ring/disc electrode, membrane conductivity cell, segmented fuel cell for current/cell voltage distributions over the active area, and gas chromatography/mass spectrometry. Because many of these diagnostics methods are not applicable or are irrelevant to foreign ions partly due to their different state (in a liquid rather than a gaseous state) and behavior (salt precipitation within the fuel cell), other diagnostic methods were employed including photography, scanning electron microscopy and energy dispersive X-ray spectroscopy. Mathematical modeling was also exploited as experimental data obtained with many in situ diagnostic methods are subject to misinterpretations because the presence of foreign ions in the membrane and ionomer affects fuel cell resistance losses that invalidate assumptions needed to separate individual performance loss contributions.

The cathode catalyst loading impact was investigated under a single set of operating conditions. The scavenging effect of liquid water was studied with an inactive fuel cell to minimize the presence of side reactions. The contaminant was carried inside the fuel cell with a saturated and inert carrier gas whereas the water was transferred from the anode compartment by thermo-osmosis [13]. Water transfer was facilitated by avoiding the use of a gas diffusion layer on the anode side. The amount of water transferred was measured by collection at the fuel cell outlet. Methanol and sulfur dioxide were used as model contaminants that either only dissolve in water or hydrolyzes and reacts to form a bisulfite ion. For methanol, outlet water samples were analyzed by cyclic voltammetry and total organic carbon. For sulfur dioxide, outlet gas samples were analyzed by gas chromatography.

RESULTS

Table 1 summarizes key metrics obtained from the in situ and ex situ diagnostic tests. Electrochemical catalyst areas and peroxide production currents indicate that the

TABLE 1. Summary of Ex Situ And In Situ Diagnostic Methods' Results for Seven Airborne Contaminants and One Foreign Cation To Resolve Contamination Mechanisms

Contaminant	Kinetic Current (% loss in air at 30°C and 0.9 V vs RHE)	Electrochemical Catalyst Area (% loss in N ₂ at 30°C)	H ₂ O ₂ Current (% gain in air at 30°C and 0.5 V vs RHE) ^a	Membrane Conductivity (% loss at 80°C and 50% relative humidity)	Dimensionless Local Current (maximum % loss and gain in air at 80°C)		Contaminant Conversion (% in air at 80°C) ^b
					Contamination Phase	Recovery Phase	
Acetonitrile	79-84 (16.9 mM)	>76 (16.9 mM)	850-1300 (16.9 mM)	0 (100 ppm), N product detected by ISE (IC tests planned)	Step change followed by a cell potential triggered evolution reaching -15 to 12 at steady state (20 ppm)	Traveling current wave reaching -28 to 22 to values approximately equal to initial values (20 ppm)	20 to 45 for 0.55 to 0.65 V (20 ppm)
Acetylene	100 (4,030 ppm)	100 (4,040 ppm)	2,700-3,800 (4,030 ppm)	1-2 (500 ppm)	Traveling current wave of -99 to 100 synchronized with voltage transient followed by -17 to 18 at steady state (300 ppm)	Step change to values approximately equal to initial values (300 ppm)	0.8 to 100 for 0.55 to 0.85 V (300 ppm)
Bromomethane	54 (400 ppm)	43 (400 ppm)	56 (400 ppm)	No ohmic loss in fuel cell	Gradual change starts after voltage steady state reaching -19 to 13 (5 ppm)	Trend continues reaching -21 to 21 (5 ppm)	0 for 0.1 to -1 V (10 ppm)
Iso-propanol	12 (1 mM)	7 (1 mM)	18 (1 mM)	No ohmic loss in fuel cell	Step change of -9 to 5 (5,300 ppm)	Reverse step change (5,300 ppm)	Not applicable
Methyl methacrylate	65 (1 mM)	43 (H _{UPD}) and 82 (PtO reduction) (1 mM)	1,300 (1 mM)	No ohmic loss in fuel cell	Step change of -7 to 6 (20 ppm)	Reverse step change (20 ppm)	49 to 57 for 0.55 to 0.68 V (20 ppm)
Naphthalene	66 (sat soln) ^c	90 (sat soln) ^c	780 (sat soln) ^c	No ohmic loss in fuel cell	Traveling current wave of -25 to 14 synchronized with voltage transient (2.3 ppm)	Traveling current wave of -39 to 40 synchronized with voltage transient (2.3 ppm)	Detectable but not quantifiable for 0.5 to 0.85 V (1.4 ppm)
Propene	53 (1,010 ppm)	26 (H _{UPD}) and ~50 (PtO reduction) (1,010 ppm)	620-960 (1,010 ppm)	No ohmic loss in fuel cell	Step change of -8 to 6 (100 ppm)	Reverse step change (100 ppm)	43 to 89 for 0.55 to 0.85 V (100 ppm)
Ca ²⁺	37 (90 mM Ca(ClO ₄) ₂), 21 (5 ppm) ^d	2 (90 mM Ca(ClO ₄) ₂), 16-46 (5 ppm) ^d	660 (90 mM Ca(ClO ₄) ₂)	1.1-11 (5 ppm) ^e	Gradual change up to -50 to 20 (5 ppm) ^f	Gradual change up to -60 to 40 (5 ppm) ^f	-

^a The total current is still mostly due to oxygen reduction in spite of a large peroxide production rate increase. ^b Observed products include: for acetonitrile, ammonia/amine; for acetylene, CO and CO₂; for iso-propanol, CO₂; for methyl methacrylate, CO₂; for naphthalene, 1,2,3,4-tetramethyl-benzene, 1,3,5,7-tetramethyl-adamantane, pentamethyl-benzene, 1-penten-3-one, 1-(2,6,6-trimethyl-1-cyclohexen-1-yl); for propene, CO₂. ^c 0.25 mM solubility at 25°C. ^d Derived from in situ polarization curve and cyclic voltammetry tests. ^e In situ result by current interrupt for 0.6-1 A cm⁻² and 125% relative humidity before a steady state is reached at 100 h. ^f 0.6 rather than 1 A cm⁻² and before a steady state is reached at 100 h. Figures in parentheses represent the contaminant concentration either in the gas phase (ppm) or liquid phase (M). Both concentration units are used for the Ca²⁺ ion. RHE – reference hydrogen electrode; GDE – gas diffusion electrode; IC – ion chromatography; ISE – ion selective electrode; TBD – to be determined; UPD – under-potential deposition.

change in kinetic resistance associated with contamination is not only due to a decrease in surface area but also to a modification of the oxygen reduction mechanism in favor of a 2 rather than a 4 electrons path leading to increased amounts of hydrogen peroxide. Only Ca²⁺ did not significantly affect the electrochemical surface area. Generally, organic contaminants undergo chemical or electrochemical reactions within the fuel cell as detected by gas chromatography/mass spectrometry analysis of outlet gases. Only bromomethane was inactive. Iso-propanol could not be analyzed because the sample gas stream drying step, which is necessary to avoid equipment damage, entrains a significant portion of iso-propanol. Ca²⁺ is not expected to be converted to Ca in the fuel cell because the electrode potentials are not sufficiently low. Acetonitrile and Ca²⁺ were the only contaminants that led to an ohmic resistance change. For acetonitrile, the change was ascribed to a decomposition product because the membrane conductivity measured ex situ was not affected

by acetonitrile. Ammonium was detected in the fuel cell outlet water. It is possible that a nitrogen organic compound is also present because the ion selective electrode cannot discriminate between such species. For Ca²⁺, ion exchange with the ionomer proton modifies ionic conductivity as well as other physico-chemical parameters. The current distribution was not affected by iso-propanol, methyl methacrylate and propene. This observation is consistent with relatively slow catalyst surface kinetics, rapid transport processes and a relatively uniform contaminant concentration across the cell. However, the other contaminants revealed varied behaviors that may be useful to facilitate mechanism identification and generalize contamination mechanisms [14]. It is hypothesized that a change in rate determining step along the contaminant transport to the catalyst surface, catalyst surface kinetics, contaminant and products transport away from the catalyst surface sequence is responsible for the change in behavior. The gas diffusion electrode water content

has not yet been measured because the increase in mass transport loss in the presence of organic contaminants was largely attributed to contaminant adsorption on the catalyst [15].

The presence of elevated levels of peroxide is expected to affect cell durability. The presence of contaminant products and the uneven current distribution may complicate performance recovery strategies.

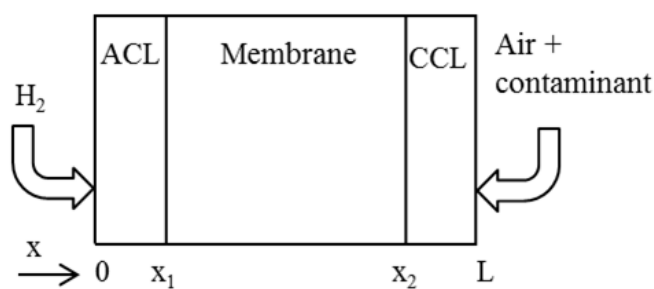
Table 2 illustrates that a 75% reduction in Pt catalyst loading from 0.4 to 0.1 mg cm⁻² leads to a decrease in cell voltage at steady state due to contamination (the difference between the cell voltage before contamination and during contamination) that generally exceeds 75% and reaches values of 92 to 6,325%. As a result, filter system specifications either need to be revised or should be determined for commercially relevant Pt catalyst loadings.

Figure 1A depicts a schematic representation of the one-dimensional (x direction) modeled membrane/electrode assembly portion. Figure 1B calculations show that the presence of a foreign cation in the catalyst layers' ionomer and membrane significantly affects the oxygen concentration distribution due to a smaller ionomer water content [16] and oxygen permeability [17]. The oxygen concentration gradient is steeper and the average oxygen concentration is lower than values in absence of foreign cation contamination. The lower oxygen concentration affects thermodynamic (Nernst equation), kinetic (oxygen reduction is a first order reaction) and mass transport contributions. The foreign cation contamination model also demonstrates that the change in oxygen permeability of the ionomer accounts for a significant fraction of the decrease in cell performance. This new information is important to focus activities aimed at minimizing the effect of foreign cation contamination on cell performance.

Figure 2A illustrates the cell and method used to measure the impact of liquid water scavenging on contaminant concentration. Figure 2B shows that the CH₃OH concentration at the cell outlet measured by two different methods acceptably fits the liquid water scavenging model over a stoichiometry range exceeding the normal operating regime of approximately 1.5 to 2.5. The same conclusion is reached from Figure 2C for the case of SO₂. However, for this particular case of a species hydrolyzing and reacting by forming a bisulfite ion, the amount of species scavenged is concentration dependent which is important for predictive

purposes. Figure 2C depicts the amount of SO₂ scavenged, which is the difference between the full line and the dash line. The amount of SO₂ scavenged increases with a decrease in inlet SO₂ concentration. Therefore, cell performance extrapolations to lower contaminant concentrations using only high concentration data while disregarding the scavenging effect are conservative.

The scavenging model reduces to a simple expression because a time-scale analysis of all relevant phenomena



ACL – anode catalyst layer; CCL – cathode catalyst layer

FIGURE 1A. Schematic polymer electrolyte membrane fuel cell representation and X-axis definition. From M.A. Uddin, U. Pasaogullari, *J. Electrochem. Soc.*, **161** (2014) F1081 (reproduced by permission of The Electrochemical Society)

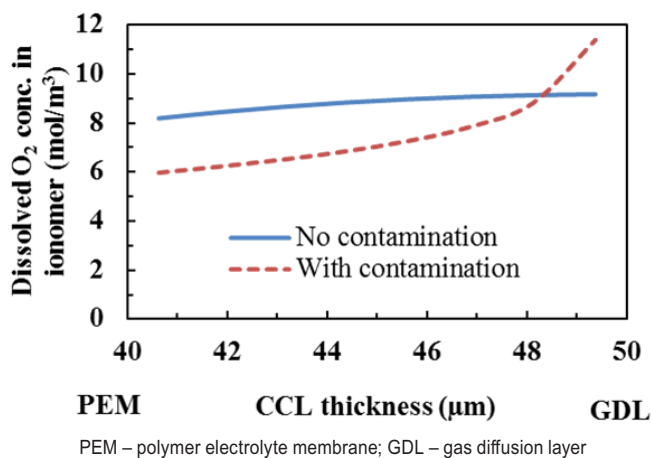
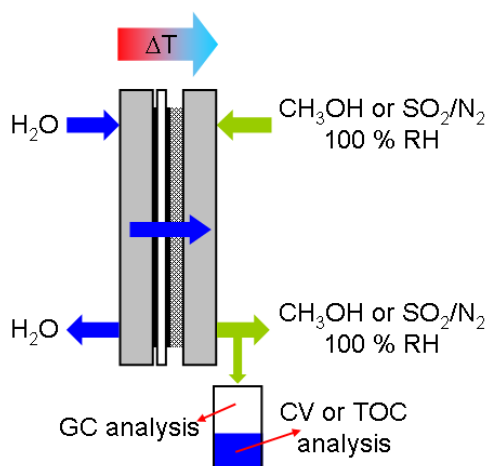


FIGURE 1B. Model predictions for the dissolved oxygen concentration profile in the CCL contaminated with Na⁺ (sulfonate site occupancy = 1 at the catalyst/GDL interface), 0.7 V, 80/100% anode/cathode relative humidity, 80°C. From M.A. Uddin, U. Pasaogullari, *J. Electrochem. Soc.*, **161** (2014) F1081 (reproduced by permission of The Electrochemical Society)

TABLE 2. Summary of the Impact of a Cathode Catalyst Loading Reduction on Steady-State Cell Performance Loss for Seven Airborne Contaminants

Contaminant	Acetonitrile	Acetylene	Bromomethane	Iso-propanol	Methyl methacrylate	Naphthalene	Propene
Cell voltage loss (% gain for a Pt loading reduction of 0.4 to 0.1 mg cm ⁻² in air at 80°C)	58 (20 ppm)	6,325 (100 ppm)	-10 (5 ppm)	92 (~8,000 ppm)	104 (20 ppm)	187 (1.4 ppm)	224 (100 ppm)



RH – relative humidity; GC – gas chromatograph; CV – cyclic voltammetry; TOC – total organic carbon

FIGURE 2A. Experimental setup schematic showing the transport of water through the PEMFC membrane/electrode assembly by thermo-osmosis, the injection of methanol and sulfur dioxide contaminants in a saturated and inert carrier gas, and the methods used to measure the amount of contaminant scavenged by liquid water. From J. St-Pierre, B. Wetton, Y. Zhai, J. Ge, *J. Electrochem. Soc.*, **161** (2014) E3357 (reproduced under the creative commons license terms, <http://creativecommons.org/licenses/by-nc-nd/4.0/>)

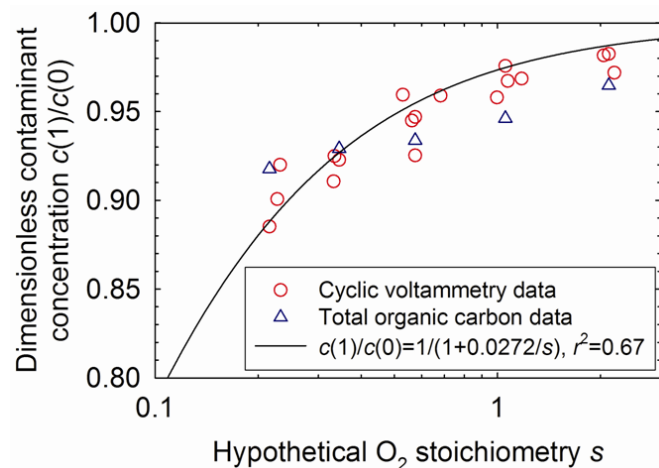


FIGURE 2B. Dimensionless methanol concentration $c(1)/c(0)$ in the PEMFC cathode outlet gas stream measured by two different methods as a function of the hypothetical oxygen stoichiometry s . $c(1)$ and $c(0)$ are respectively the cell outlet and inlet concentrations. The full line represents a curve fit to the mathematical model. Dimensionless contaminant inlet concentration c_{in}/c_a approximately 1,000 ppm methanol in N_2 , 80°C, 48.3 kPag, 100% inlet relative humidity, $c_r = 34.9 \text{ mol m}^{-3}$. From J. St-Pierre, B. Wetton, Y. Zhai, J. Ge, *J. Electrochem. Soc.*, **161** (2014) E3357 (reproduced under the creative commons license terms, <http://creativecommons.org/licenses/by-nc-nd/4.0/>)

revealed that liquid water accumulation within the cell is the slowest step. As a result, the liquid water is saturated by the contaminant, which simplified model derivation by eliminating the need to track individual water droplets. The

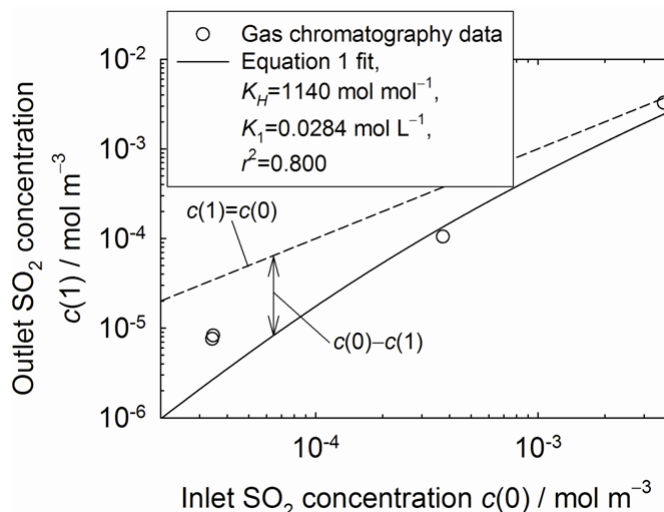


FIGURE 2C. SO_2 concentration $c(1)$ in the PEMFC cathode outlet gas stream as a function of contaminant inlet concentration $c(0)$ at a hypothetical oxygen stoichiometry s of approximately 2.5. 80°C, 48.3 kPag, 100% inlet relative humidity, $c_r = 34.9 \text{ mol m}^{-3}$. $K_H = 1,140 \text{ mol mol}^{-1}$ ($H = 0.021 \text{ m}^3 \text{ mol}^{-1}$), $K_1 = 0.0284 \text{ mol L}^{-1}$ ($H' = 0.00324 \text{ m}^{3/2} \text{ mol}^{-1/2}$) for equation 1. From J. St-Pierre, B. Wetton, Y. Zhai, J. Ge, *J. Electrochem. Soc.*, **161** (2014) E3357 (reproduced under the creative commons license terms, <http://creativecommons.org/licenses/by-nc-nd/4.0/>)

model expression, which depends on two dimensionless parameters is simple which facilitates its use to calculate effective concentrations and improve correlations with cell performance losses:

$$\frac{c(x)}{c(0)} = \left(\frac{-W_2 x}{1+W_1 x} + \sqrt{\frac{W_2^2 x^2}{(1+W_1 x)^2} + \frac{1}{1+W_1 x}} \right)^2, c(0) = \frac{c_{in} c_r}{c_a} \quad (1)$$

where c is the molar concentration of contaminant X in the gas phase (mol m^{-3}), x the dimensionless flow field channel length, c_{in} the inlet contaminant X concentration in the ambient air on a dry basis (mol m^{-3}), c_r the molar concentration of non vapor gases at saturation conditions within the fuel cell (mol m^{-3}), c_a the molar concentration of an ideal gas at a pressure of 1 atmosphere (mol m^{-3}), W_1 represents the dimensionless number characterizing the severity of the liquid water scavenging effect on the contaminant X, and W_2 represents the dimensionless number characterizing the severity of the liquid water scavenging effect on the contaminant X in the presence of dissociation reactions.

CONCLUSIONS AND FUTURE DIRECTIONS

- Contamination mechanisms for seven airborne contaminants and one foreign cation were refined by building a database using a variety of ex situ and in situ diagnostic methods

- The performance loss at steady state due to contamination is generally and proportionally larger than the decrease in cathode catalyst loading thus suggesting a revision of filter system specifications for commercially relevant low catalyst loadings
- For foreign cation contamination, the performance loss associated with the decrease in oxygen permeability through the ionomer is significant and cannot be ignored to minimize its impact
- Contaminant scavenging by liquid water was demonstrated and modeled to improve correlations between fuel cell performance losses and the effective contaminant concentration
- Complete long-term tests to assess the impact of increased peroxide production in the presence of airborne contaminants on fuel cell durability
- Develop mitigation strategies for the most important contaminants
- Continue to disseminate the large fuel cell contamination database

FY 2014 PUBLICATIONS/PRESENTATIONS

1. J. Ge, J. St-Pierre, Y. Zhai, 'PEMFC Cathode Catalyst Contamination Evaluation with a RRDE – Methyl Methacrylate', *Int. J. Hydrogen Energy*, accepted.
2. M.A. Uddin, U. Pasaogullari, 'Computational Modeling of Foreign Cation Contamination in PEFCs', *J. Electrochem. Soc.*, **161** (2014) F1081.
3. J. Ge, J. St-Pierre, Y. Zhai, *Electrochim. Acta*, **138** (2014) 437.
4. J. Ge, J. St-Pierre, Y. Zhai, *Electrochim. Acta*, **134** (2014) 272.
5. J. Ge, J. St-Pierre, Y. Zhai, *Electrochim. Acta*, **133** (2014) 65.
6. J. St-Pierre, B. Wetton, Y. Zhai, J. Ge, *J. Electrochem. Soc.*, **161** (2014) E3357.
7. X. Wang, J. Qi, O. Ozdemir, A. Uddin, U. Pasaogullari, L. J. Bonville, T. Molter, *J. Electrochem. Soc.*, **161** (2014) F1006.
8. J. St-Pierre, M. Angelo, K. Bethune, J. Ge, S. Higgins, T. Reshetenko, M. Virji, Y. Zhai, 'PEMFC Contamination – Fundamentals and Outlook', *Electrochem. Soc. Trans.*, accepted.
9. M.A. Uddin, X. Wang, M.O. Ozdemir, J. Qi, L. Bonville, U. Pasaogullari, T. Molter, 'Distributed PEFC Performance during Cationic Contamination', *Electrochem. Soc. Trans.*, accepted.
10. M.A. Uddin, J. Qi, X. Wang, M.O. Ozdemir, N. Khajeh-Hosseini-Dalasm, L. Bonville, U. Pasaogullari, T. Molter, 'Study of Through Plane Cation Contamination in Polymer Electrolyte Fuel Cell', *Electrochem. Soc. Trans.*, accepted.
11. Y. Zhai, J. St-Pierre, J. Ge, 'PEMFC Cathode Contamination Evaluation with Membrane Conductivity Cell, CA, CP, CV, EIS, GC/MS and ISE – Acetonitrile', *Electrochem. Soc. Trans.*, accepted.
12. M.A. Uddin, X. Wang, J. Qi, M.O. Ozdemir, L. Bonville, U. Pasaogullari, T. Molter, 224th Electrochemical Society meeting oral presentation, abstract 1334.
13. J. Qi, X. Wang, M.O. Ozdemir, M.A. Uddin, L. Bonville, U. Pasaogullari, T. Molter, 224th Electrochemical Society meeting oral presentation, abstract 1333.
14. X. Wang, J. Qi, O. Ozdemir, U. Pasaogullari, L.J. Bonville, T. Molter, 224th Electrochemical Society meeting oral presentation, abstract 1332.
15. J. St-Pierre, J. Ge, Y. Zhai, T. Reshetenko, M. Angelo, 224th Electrochemical Society meeting oral presentation, abstract 1330.
16. Y. Zhai, J. St-Pierre, J. Ge, 224th Electrochemical Society meeting oral presentation, abstract 1329.
17. T. Reshetenko, J. St-Pierre, 224th Electrochemical Society meeting oral presentation, abstract 1328.
18. J. Ge, Y. Zhai, J. St-Pierre, 224th Electrochemical Society meeting oral presentation, abstract 1302.
19. J. St-Pierre, 'The Effect of Airborne Contaminants on Fuel Cell Performance and Durability', USDRIVE Fuel Cell Tech Team meeting oral presentation, Southfield, MI, January 15, 2014.
20. J. St-Pierre, M. Angelo, K. Bethune, J. Ge, S. Higgins, T. Reshetenko, M. Virji, Y. Zhai, 225th Electrochemical Society meeting oral presentation, abstract 796.
21. M.A. Uddin, X. Wang, M.O. Ozdemir, J. Qi, L. Bonville, U. Pasaogullari, T. Molter, 225th Electrochemical Society meeting oral presentation, abstract 638.
22. M.A. Uddin, J. Qi, X. Wang, M.O. Ozdemir, N.K.H. Dalasm, L. Bonville, U. Pasaogullari, T. Molter, 225th Electrochemical Society meeting oral presentation, abstract 637.
23. J. St-Pierre, 'PEMFC Contamination – Fundamentals and Outlook', General Motors oral presentation, Pontiac, MI, June 9, 2014.
24. J. St-Pierre, 'PEMFC Contamination – Fundamentals and Outlook' and 'The Effect of Airborne Contaminants on Fuel Cell Performance and Durability', SAE International oral presentations, Troy, MI, June 10, 2014.
25. J. St-Pierre, 'The Effect of Airborne Contaminants on Fuel Cell Performance and Durability', United States Department of Energy 2014 Annual Merit Review meeting oral presentation, Washington, DC, June 18, 2014.

REFERENCES

1. J. St-Pierre, 'Air Impurities', in *Polymer Electrolyte Fuel Cell Durability*, Edited by F.N. Büchi, M. Inaba, T.J. Schmidt, Springer, 2009, p. 289.
2. J. St-Pierre, M. Angelo, K. Bethune, J. Ge, S. Higgins, T. Reshetenko, M. Virji, Y. Zhai, 'PEMFC Contamination – Fundamentals and Outlook', *Electrochem. Soc. Trans.*, accepted.
3. J. St-Pierre, Y. Zhai, M.S. Angelo, *J. Electrochem. Soc.*, **161** (2014) F280.
4. J. St-Pierre, Y. Zhai, M. Angelo, *Int. J. Hydrogen Energy*, **37** (2012) 6784.

5. J. St-Pierre, Y. Zhai, J. Ge, M. Angelo, T. Reshetenko, T. Molter, L. Bonville, U. Pasaogullari, W. Collins, S. Wessel, DOE Hydrogen and Fuel Cells Program, FY 2013 Annual Progress Report, p. V-3.
6. B. L. Kienitz, H. Baskaran, T.A. Zawodzinski Jr., *Electrochim. Acta*, **54** (2009) 1671.
7. B. Kienitz, B. Pivovar, T. Zawodzinski, F.H. Garzon, *J. Electrochem. Soc.*, **158** (2011) B1175.
8. M.F. Serincan, U. Pasaogullari, T. Molter, *Int. J. Hydrogen Energy*, **35** (2010) 5539.
9. J. St-Pierre, *Int. J. Hydrogen Energy*, **36** (2011) 5527.
10. J. St-Pierre, *J. Power Sources*, **196** (2011) 6274.
11. T. Okada, J. Dale, Y. Ayato, O.A. Asbjørnsen, M. Yuasa, I. Sekine, *Langmuir*, **15** (1999) 8490.
12. T. Okada, Y. Ayato, J. Dale, M. Yuasa, I. Sekine, O.A. Asbjørnsen, *Phys. Chem. Chem. Phys.*, **2** (2000) 3255.
13. R. Zaffou, J.S. Yi, H.R. Kunz, J.M. Fenton, *Electrochem. Solid-State Lett.*, **9** (2006) A418.
14. T.V. Reshetenko, K. Bethune, M.A. Rubio, R. Rocheleau, *J. Power Sources*, **269** (2014) 344.
15. J. St-Pierre, J. Ge, Y. Zhai, T.V. Reshetenko, M. Angelo, *Electrochem. Soc. Trans.*, **58**(1) (2013) 519.
16. K. Hongsirakarn, J.G. Goodwin Jr, S. Greenway, S. Creager, *J. Power Sources*, **195** (2010) 7213.
17. K. Broka, P. Ekdunge, *J. Appl. Electrochem.*, **27** (1997) 117.